Nugraha *et al.* 2024 | Vol. 2: 24 – 35
publishing.ssrs.or.id/ojs

SSRS Journal B: Spatial Research

Research Article **Open Access**

Investigating the Impact of the Tsunami at Handeleum Island Resort, Ujung Kulon National Park Using Geospatial Technology

Eka Sartika Nugraha[1,2], Abd. Malik A. Madinu[1,2,3], Salamah Zukhrufa Jannah[1,2], Tarisa Hikmah Ameiliani[2,4], Rahmat Asy'Ari[2,3,4], Faradilla Anggit Prameswari[5], Moh Zulfajrin[6,7], Lina Lathifah Nurazizah[6,7], Made Chandra Aruna Putra[2,8], Zayyaan Nabila Khairunnisa[2,9], Azelia Dwi Rahmawati[2,4], Yudi Setiawan[10,11], Anggodo[12]

[1] *Undergraduate Student, Department of Geophysics and Meteorology, Faculty of Mathematics and Natural Science (FMIPA), IPB University, IPB Dramaga Campus, Bogor Regency 16680, Indonesia*
[2] *IPB Sustainable Science Research Students Association (IPB SSRS Association), IPB University, Bogor Regency 16680, Indonesia*
[3] *SSRS EarthInformatics Labs, SSRS Institute – SSRS Group, Bogor Regency, West Java, Indonesia*
[4] *Undergraduate Student, Department of Forest Management, Faculty of Forestry and Environment, IPB University, IPB Dramaga Campus, Bogor Regency 16680, Indonesia*
[5] *Undergraduate Student, Department of Geography, Faculty of Mathematics and Natural Science (FMIPA), University of Indonesia, Depok Regency 16424, Indonesia*
[6] *Computational Soil Science Research Group - IPB University, Faculty of Agriculture, IPB University, Bogor Regency 16680, Indonesia*
[7] *SSRS Banggai Advanced Research Facility, SSRS Institute – SSRS GroupBanggai Regency, Indonesia*
[8] *Undergraduate Student, Department of Marine Science and Technology, Faculty of Fisheries and Marine Science, IPB University, Bogor Regency 16680, Indonesia*
[9] *Undergraduate Student, Department of Civil and Environmental Engineering, Faculty of Agricultural Technology, IPB University, Bogor Regency 16680, Indonesia*
[10] *Department of Forest Resources Conservation and Ecotourism, Faculty of Forestry and Environment, IPB University, Bogor Regency 16680, Indonesia*
[11] *Center for Environmental Science, Lembaga Penelitian dan Pemberdayaan Masyarakat IPB, IPB University, Bogor Regency 16680, Indonesia*
[12] *Ujung Kulon National Park (UKNP), Ministry of Environment and Forestry, Pandeglang, Banten 42264, Indonesia*

* Correspondence: ekasartika_nugraha@apps.ipb.ac.id

Abstract: Natural disasters are events that often occur anywhere and anytime. The tsunami natural disaster is a tidal wave disaster generated by tectonic earthquakes, volcanic eruptions in the ocean, or landslides that can cause damage, loss and even take lives. Ujung Kulon National Park (UNKT) is one of 12 existing national parks on the island of Java and is home to key species of the Java plain. Biodiversity in the national park is threatened by the volcanic activity of Anak Krakatau. The most recent activity generated a tsunami wave in 2018 that damaged most of the coastal forest ecosystems on the northern Ujung Kulon peninsula. The geographical condition of UNKT which varies from flat, sloping, wavy, hilly, to mountainous, causes the high flora and fauna in the area. The tsunami event will cause considerable damage, especially to the flora and fauna in the area. Affected areas are identified and evaluated using a comparison of the vegetation index Normalized Difference Vegetation Index (NDVI), Modified Normalized Difference Vegetation Index (MNDVI), Enhanced Vegetation Index (EVI), Soil Adjusted Vegetation Index (SAVI), Atmospherically Resistant Vegetation Index (ARVI), Specific Leaf Area Vegetation Index (SLAVI), and Green Normalized Difference Vegetation Index (GNDVI), the water index is Augmented Normalized difference water index (ANDWI), Modified Normalized Difference Water Index (MNDWI), and Land Surface Water Index (LSWI), and the Normalized Difference Built-up Index (NDBI) and Index-Based Built-up Index (IBI). The classification shows that there are 1.268,53 ha (1,06% of the total conservation area). The analysis shows that the tsunami had a negative impact on the coastal forest vegetation on the Ujung Kulon peninsula as well as the surrounding settlements. Therefore, these problems need special attention, especially in the UKNT ecosystem. This study is expected to be a consideration for the management of the UKNT area in order to preserve the existing ecosystem to protect the endangered Javan Rhino.

Keyword: Tsunami, Ujung Kulon National Park, geospatial, indices

Nugraha ES, Madinu AMA, Jannah SZ, Ameiliani TH, Asy'Ari R, Prameswari FA, Zulfajrin M, Nurazizah LL, Putra MCA, Khairunnisa ZN, *et al.*. 2024. Investigating the impact of the tsunami at Handeleum Island Resort, Ujung Kulon National Park using geospatial technology. *SSRS Journal B: Spatial Research*. 2: 24 - 35

INTRODUCTION

A natural disaster is a sudden and massive biophysical phenomenon on Earth that results in the loss of life, assets, or both (Rajan *et al.* 2021). Tsunamis represent one of the most significant categories of natural disasters globally. The tsunami will pose increasingly complex challenges for society. Such events may be triggered by other hazards, including earthquakes, landslides, and volcanoes (Rafliana *et al.* 2022). A tsunami of considerable magnitude, reaching a maximum height of 13 meters (Muhari *et al.* 2019), was generated in the Sunda Strait, Indonesia, as a consequence of volcanic activity at Mount Anak Krakatau on the night of December 22, 2018. The impact of the tsunami on the islands surrounding the Anak Krakatau volcano is evidenced by the destruction of coastal forests (Muhari *et al.* 2019). Further tsunami impacts were observed in a natural area designated for rhino conservation on the Ujung Kulon Peninsula located about 60 km south of the AK volcano. The tsunami greatly impacted the 4.5 km coastline where coastal forests were completely washed away to a distance of up to 800 m inland (Muhari *et al.* 2019).

Remote sensing is an effective tool for realizing synoptic drought monitoring over large areas due to near real-time observation capacity with high Spatio-temporal resolution (Wardlow *et al.* 2012). Remote sensing technology has evolved rapidly in recent years thus improving the ability to capture geographical images at high resolution and in detail. Remote sensing images are taken from a height and capture a very large area compared to natural images (Zia *et al.* 2022). After the occurrence of a natural disaster, it is necessary to have the necessary information to understand the extent of the damage and to provide information on recovery strategies. Remote sensing can be a source of information, especially when areas are difficult to access physically (Marlier *et al.* 2022). Cloud computing since they were developed to integrate geospatial data and services with web-based applications so that they are cloud-ready (McKee *et al.* 2011).

The index algorithm is one of many used in the character of the land cover by utilizing the wavelength read by satellite sensors. The vegetation index is a common indicator for analyzing phonological features and has been used extensively in investigative and dynamic change (Li *et al.* 2021). There are various types of vegetation indexes, such as the Zeng *et al.* (2022) involving the DVI, RVI, NDVI, GNDV, NDTI, CRVI, SSVI, GVI, WET, EVI, SAVI, LSWI overcoming the traditional limits of the salt marsh-swamp classification method, and achieving a semi-automatic identification and extraction of various salt marshal-swamp vegetation communities in the Bohai sea coast of China. The use of vegetation indices has been commonly used in remote sensing, for example urban dynamics research (Rivai *et al.* 2023), coastline change (Madinu *et al.* 2024;

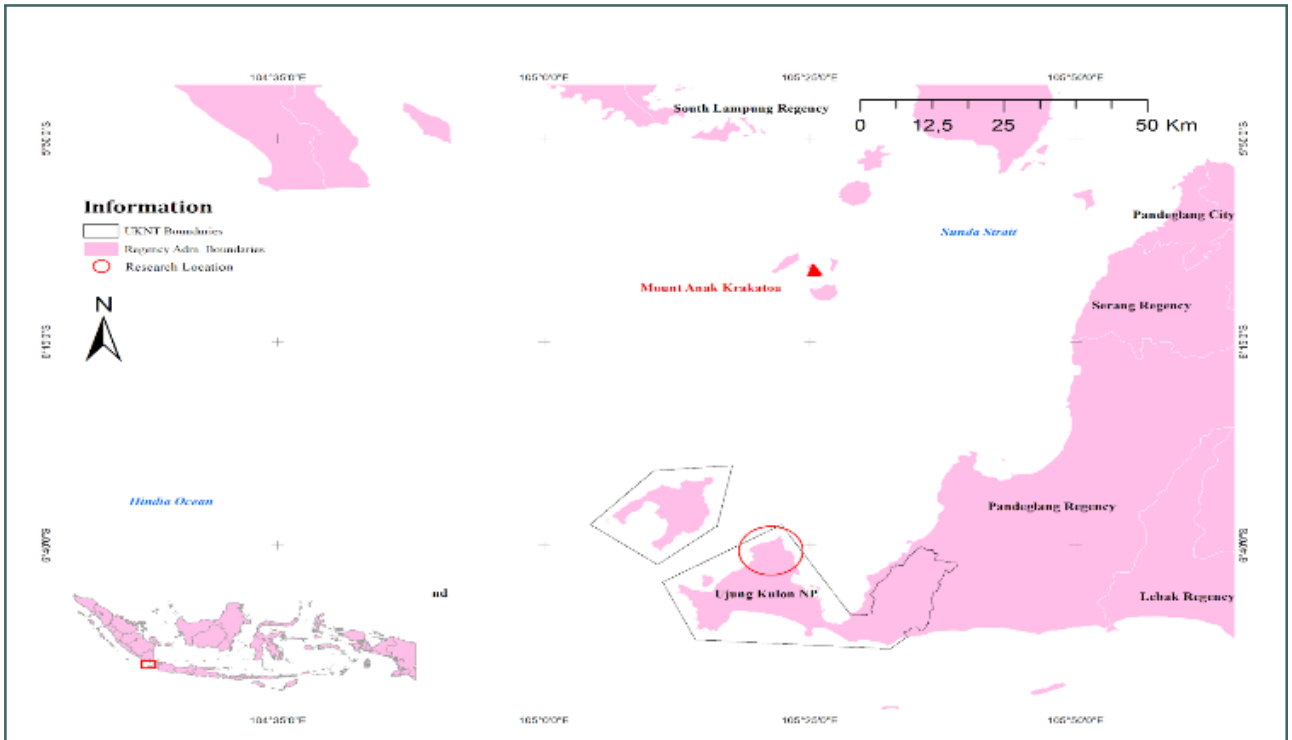

Figure 1. Research location

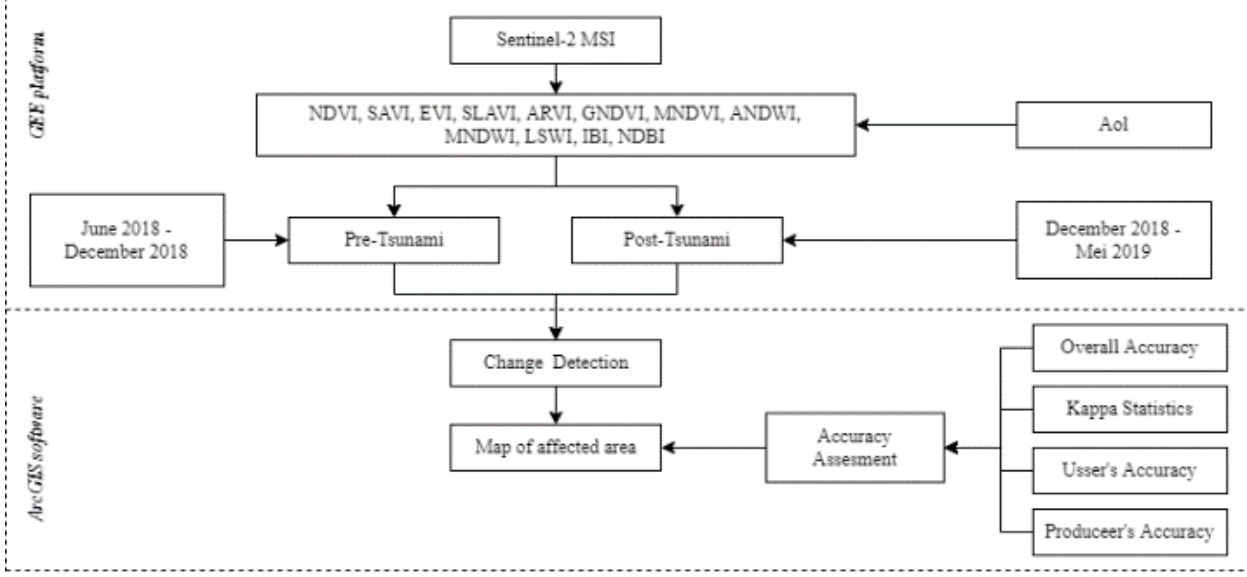

Figure 2. Research flowchart

Asy'Ari *et al.* 2023A), mangrove carbon stock (Adni *et al.* 2024), agriculture in national park area (Wandani *et al.* 2023), and LULC (Asy'Ari et al. 2023B; Alwysihah *et al.* 2023).

Information about the tsunami's impact is very important as an evaluation and recovery plan for the affected area. The application of geospatial technology to the process of analyzing affected land is one of the activities that show efforts to monitor the area around the National Park. Therefore, research on the impact of the tsunami in Ujung Kulon National Park (UKNP) was carried out to investigate the impact of the tsunami. This research is expected to be used as a consideration for decision-makers and also for future research.

METDHOLOGY

Research Location

Handeuleum Island is located on the Ujung Kulon Peninsula in the northern part of Banten, adjacent to the Krakatau Nature Reserve. UKNP has status as a World Heritage Site and has rich and valuable biodiversity (Marine Conservation Areas in Southeast Asia 2005). Besides having high biodiversity, it also has the largest remaining lowland rainforest area in the plains of Java (UNESCO-WHC). The 123.000 ha park was first designated a nature reserve in 1921 and became a national park in 1980 (Wells *et al.* 1999). Endangered species of plants and animals can be found there, one of which is the Javan Rhino (UNESCO-WHC). 40% of this area is a marine area (Indonesian Nature).

Research Procedures

This study used primary data derived from the Sentinel 2 Multispectral Instrument (MSI) satellite. Sentinel-2 is an earth-level monitoring satellite launched by ESA (European Space Agency). The ability to identify the earth's surface with the ability of sensors that produce medium-resolution images of 10 - 60 meters (Drusch *et al.* 2012). The Sentinel-2 satellite has two probes namely Sentinel-2A and Sentinel-2B which were launched to improve the temporal resolution of these satellites (Navarro *et al.* 2017). This method of detecting changes has been carried out before and refers to the research of Seydi *et al.* (2021) to find out the areas affected by fires. And also this method was carried out by Sambah and Miura (2016) which involved the NDVI and NDWI index algorithms to identify the impact of the tsunami in Japan.

This research took place from June 2018-December 2018 (Pre-Tsunami) to December 2018-May 2018 (Post Tsunami). Analysis of satellite imagery data involves two main components, namely Google Earth Engine (GEE) and ArcMap Software (Figure 2). The GEE platform will input MSI's Sentinel-2 image and classify it according to a predefined index. This platform is a cloud computing-based geospatial technology that offers many conveniences (Mutanga and Kumar 2019). Kumar and Mutanga (2018) explain that the platform is integrated with various satellite

imagery resources and is often used in various analyses of the earth's surface. According to Gorelick *et al.* (2017), this geospatial platform uses Google's storage resources so that it can perform geospatial analysis up to a global scale. The indices determined in this study include vegetation index, built-up land, and water index.

Table 1. List of vegetation indexes involved

No	Method	Formula	Reference
1	Normalized Difference Vegetation Index (NDVI)	NDVI = NIR - Red / NIR + Red	Rouse jr. 1973
2	Modified Normalized Difference Vegetation Index (MNDVI)	MNDVI = (Red Edge 2 - Red Edge 1) / (Red Edge 2 + Red Edge 1)	Jurgens 1997
3	Enhanced Vegetation Index (EVI)	EVI = G ((NIR - Red) / (NIR + C1 x Red - C2 x Blue + L))	Huete *et al.* 2002
4	Soil Adjusted Vegetation Index (SAVI)	SAVI = 1.5 (NIR - Red)/ (NIR + Red + 0.5)	Huete 1988
5	Atmospherically Resistant Vegetation Index (ARVI)	ARVI = (NIR - (Red - (Blue - Red))) / NIR + (Red - (Blue - Red)))	Kauffman dan Tanre 1992
6	Specific Leaf Area Vegetation Index (SLAVI)	SLAVI = NIR / (Red + SWIR)	Lymburner *et al.* 2000
7	Green Normalized Difference Vegetation Index (GNDVI)	GNDVI = (NIR - Green) / (NIR + Green)	Gitelson *et al.* 1996

Furthermore, data processing is carried out using ArcMap software with the aim of determining the distribution of damage to areas affected by the tsunami. The distribution of area damage was analyzed using an index algorithm capable of reading the difference in land cover on the earth's surface through wavelengths. Rees (1999) explained that various index algorithms are affected, especially the vegetation index, which was created to help identify vegetation on the earth's surface.

Data Analysis

Several indices were used in this study to detect the impact of tsunami damage in the study area. The indexes are selected based on their function and used according to the characteristics of the affected area. Some of the indices used in this research are vegetation index (NDVI, MNDVI, EVI, SAVI, ARVI, SLAVI, GNDVI) (Table 1), water index (ANDWI, MNDWI, and LSWI) (Table 2), and built-up land index (NDBI, and IBI) (Table 3). The detection process can be seen through the following flow chart. The index used is presented in the table below.

Table 2. List of water indexes involved

No	Method	Formula	Reference
1	Augmented Normalized difference water index (ANDWI)	ANDWI = (Blue + Green + Red - NIR - SWIR1 - SWIR2) / (Blue + Green + Red + NIR + SWIR1 + SWIR2	Rad *et al.* 2021
2	Modified Normalized Difference Water Index (MNDWI)	MNDWI = (Green - SWIR1) / (Green - SWIR1)	Xu 2006
3	Land Surface Water Index (LSWI)	LSWI = (NIR - SWIR) / (NIR + SWIR)	Xiao *et al.* 2002

Table 3. List of built-up indexes involved

No	Method	Formula	Reference
1	Index-Based Built-up Index (IBI)	IBI = ((NIR)/NIR + Red)) + ((Green)/Green + SWIR1))	Xu 2008
2	Normalized Difference Built-up Index (NDBI)	NDBI = (SWIR - NIR) / (SWIR + NIR)	Zha *et al.* 2003

Accuracy measurement

Detection results using a remote sensing approach often produce spatial information that does not match the actual conditions. It is necessary to carry out systematic testing to test the level of accuracy of the results obtained through accuracy measurement (Foody 2004; Rwanga and Ndambukti 2017). In addition, these measurements were treated before spatial information from the study was disseminated to users (Congalton and Green 2009). This is a determinant of the quality of the data produced. This study involves accuracy analysis, such as Overall Accuracy (OA; a), Kappa Statistics (KS; b), User Accuracy (UA; c), and Producer Accuracy (PA; d). This accuracy test involves validation data with a total of 100 data captured through detailed imagery on the Google Earth Pro platform. The calculation of this analysis is by testing all tsunami detection results from various indices so as to obtain an index that has a high level of accuracy. The test results through the KS formula refer to the class of interpretation of values in Table 4 hat have been created before and become the most common in testing the accuracy level of data.

$$\text{Overall Accuracy (OA)} = \frac{1}{N}\sum_{i=1}^{r} X_{ii} \times 100\% \quad \text{..... (a)}$$

$$\text{Kappa Statistics} = \frac{N\sum_{i=1}^{r} X_{ii} - \sum_{i=1}^{r} X_{ii}\,(X_{i+} \times X_{+i})}{N^2 - \sum_{i=1}^{r} X_{ii}\,(X_{i+} \times X_{+i})} \quad \text{.....(b)}$$

$$\text{User's Accuracy} = \frac{X_{ii}}{X_{+i}} \times 100\% \quad \text{.....(c)}$$

$$\text{Producer's Accuracy} = \frac{X_{ii}}{X_{i}} \times 100\% \quad \text{.....(d)}$$

Table 4. Interpretation of kappa values

Kappa value	Information
<0.00	Poor
0.00 – 0.20	Slight
0.21 – 0.40	Fair
0.41 – 0.60	Moderate
0.61 – 0.80	Substantial
0.81 – 1.00	Almost perfect

RESULTS AND DISCUSSION

Tsunami area in UKNP

The study site is a sensitive area that has the status of a conservation forest with certain functions and purposes. The location of this study is included in the management of the UKNP area, namely the Handeuleum Island Resort and is located on the northern peninsula of the Ujung Kulon National Park beach. Ujung Kulon National Park (UKNP) is one of 12 national parks established on Java Island and is home to a key species of the Java plain. UKNP has been a nature reserve since 1921 and belongs to the National Park of the same name since 1980. According to Hommel (1987). UKNP is an important conservation area because of its Javan rhino population which may be an area with one of the remaining in the world. The existence of other valuable species such as bulls, javanese deer, leopards, javan gibbons, javanese tigers, and the beauty of the scenery. UKNP is located in the western part of the island of Java, Indonesia and is an area that includes mount Krakatau and several small islands around it, one of which is the island of Handeleum. Biodiversity in this national park is threatened by the volcanic activity of Mount Anak Krakatau. The last activity that resulted in a tsunami in 2018 damaged most of the coastal forest ecosystems on the northern Ujung Kulon Peninsula (Figure 3).

Figure 3. Tsunami impact in Ujung Kulon National Park (UKNP)

Tsunami Detection Result

The tsunami had a devastating impact on the land in UKNP. Siripong (2006) explains that tsunamis produce impacts such as coastal sand erosion and the enlargement of waterways. The impact of the tsunami that changed the landscape around the coast is momentum to quickly detect the extent of the damaging impact using satellite imagery (Koshimura *et al.* 2020; Sambah and Miura 2016). This is one of the properties of the tsunami that can damage the landscape. In addition, the tsunami that occurred in this national park was a tsunami disaster due to volcanic activity from Mount Anak Krakatau. Singh et al. (2014) explained that large and powerful earthquakes have a major impact to create tsunami waves. However, in this case, the tsunami was caused by the ruins of one of the sides of the Anak Krakatau mountain. Damage occurs along coastal forests and to the north of this national park. Such as sand erosion can be seen from the mechanism

of utilizing wavelength differences in the same place so as to provide spatial-based information.

Table 5. Distribution of tsunami damage based on several indices used

No	Index	Extent of damage		Accuracy	
		Area (ha)	Percentage (%)	OA (%)	KS
1	MNDVI	207,01	0,16	93,00	0,87
2	EVI	1.268,53	1,06	93,00	0,87
3	ARVI	3.291,13	2,67	79,00	0,65
4	SLAVI	235,11	0,19	94,00	0,89
5	GNDVI	254,69	0,20	79,00	0,64
6	ANDWI	6.269,35	5,09	48,89	0,31
7	MNDWI	435,88	0,35	98,00	0,96
8	LSWI	415,61	0,33	89,00	0,80
9	IBI	606,65	0,49	44,00	0,26
10	NDBI	667,50	0,54	82,00	0,68
11	SAVI	272,82	0,22	94,00	0,89
12	NDVI	220,37	0,17	94,00	0,89
Average		661,50	0,57	82,32	0,73

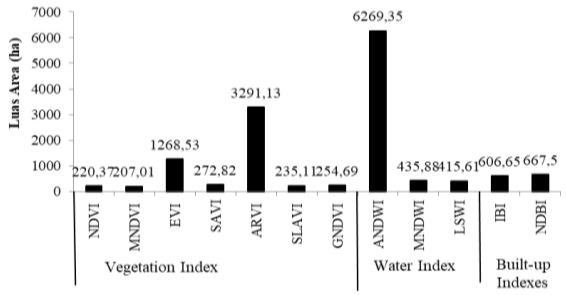

Figure 4. Graph of the difference in the detection results of each index

Three types of indices are involved, namely the vegetation, water, and land-building type indices to detect this disaster, and are presented in (Table 2) and (Figure 4). The results of the damage detection analysis of each index show that the Tsunami has an impact on land use change. In this study, the affected area was shown by the red color (Figure 5). The spatially visualized damage area (Figure 5) shows that the area affected by the damage is in the northern part which tends to be red in all indices. The results of the analysis show that the damage caused by the tsunami tends to be in the water area shown by the ANDWI index. The ANDWI Index is a water index that produces the highest damage area of 6269.35 or around 5.09% of the total area of UKNP. While the damage shown by the EVI index is 1.2 68.53 ha or equivalent to 1.06% of the research area.

MNDVI, SLAVI, GNDVI, SAVI, and NDVI have an area value of approximately 207 - 272 ha. The vulnerable value is the result of the detection of the vegetation type index and is different from the water type index which has a higher area value. For example, MNDWI and LSWI have detected area values of 435.88 ha and 415.61 ha, respectively. A small percentage of the results of these two indices are spatially distributed in areas of the ocean that should not have changed (Figure 5: Parts I and J). Muhari *et al.* (2019) explained that the tsunami released from the direction of Mount Anak Krakatau hit the peninsula at the end of the kulon to destroy natural forests about 800 meters from the coast. From the various indices involved, it provides losses to national park managers in an effort to save coastal forests in conservation forest areas. The loss of coastal forests north of the national park is an evaluation of all programs launched in saving rare species of Javan rhinoceros and another biodiversity. Controlling the impact of this tsunami can be done by creating natural fortifications such as planting mangroves along the coast that are often or potentially affected by tsunamis (Alongi 2008).

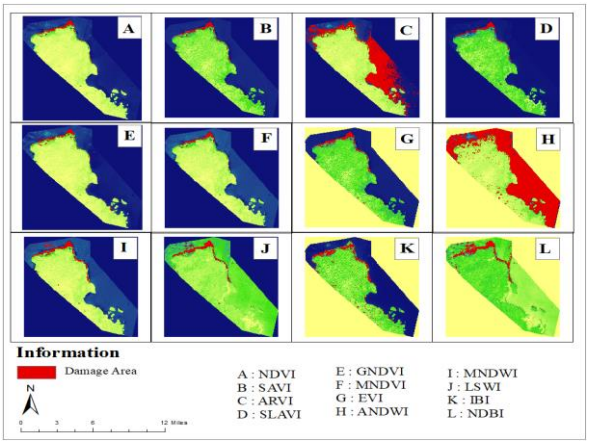

Figure 5. Spatial distribution of the results of the distribution of each index

Characteristics of index for Tsunami detection

Index characteristics can be judged by the wavelengths reflected by the earth's surface, especially in areas that have undergone changes (Sugianto and Rusdi 2017). In general, indessx algorithms are launched with different functions according to the shape and physical characteristics of the earth's surface. All indices are directed to assess changes due to the tsunami. Particularly formed vegetation indices with the aim of identifying plants on the surface of the earth.

Rouse jr *et al.* (1973) launched the NDVI index in 1973 with the aim of assisting in identifying and monitoring vegetation on the earth's surface. NDVI values are represented in ratios that range from -1 to 1. If explored deeply, extreme negative values represent water, values around zero represent barren land, and values above 0.2 represent green vegetation. Until now, the NDVI index has been used in various rapid identification cases related to plants, including monitoring vegetation damage due to tsunami malignancy. Such as Jiji *et al.* (2019) which involves this index on vegetation segments so that it can help in identifying areas of damage due to tsunamis. Figure 6 shows the differences in areas affected by the tsunami and is scattered along the coast and shown in bluish-green color. This is because the NDVI index has a level of sensitivity to the components of vegetation, water, and open ground. This can be shown by the very serious changes in the forest vegetation of the national park due to exposure to tsunami waves and also the content of seawater that submerges vegetation on land. Referring to Maher *et al.* (2015) explained that the NDVI index relies on plant chlorophyll so that it can determine the level of plant health.

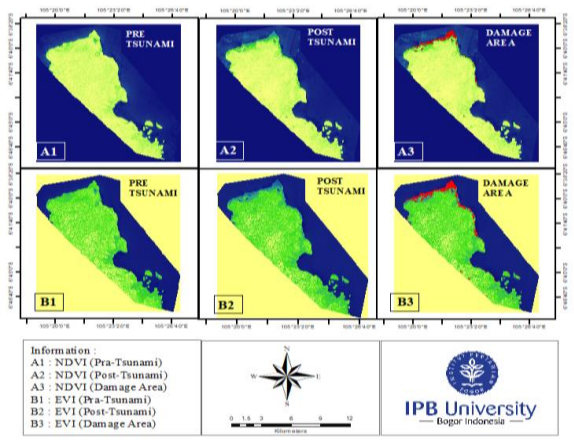

Figure 6. Index Assessment NDVI and EVI

The NDVI and EVI indices were used to compare the ability to detect differences in vegetation density conditions during the pre-tsunami, post-tsunami, and area damage periods. NDVI can be used to measure at various spatial scales how changes in vegetation distribution, phenology, and productivity will affect upper trophic levels (Pettorelli *et al.* 2005). Vegetation density decreased after the tsunami as shown in red (damage area). This can be seen in Figure 6 which shows the development of changes in the composition of vegetation density levels spatially and temporally. Somvansi and Kumari (2020) explain that the EVI index is more responsive to the variety, type, and architecture of the canopy. This makes it easier for the index to detect changes that occur in the forest landscape. The EVI index in some cases is also used in identifying vegetation changes that occur on the earth's surface. For example, Andersson *et al.* (2015) involved the EVI index in detecting the recovery from the impact of the Indian Ocean tsunami natural disaster. These two indices show how the tsunami affects vegetation density.

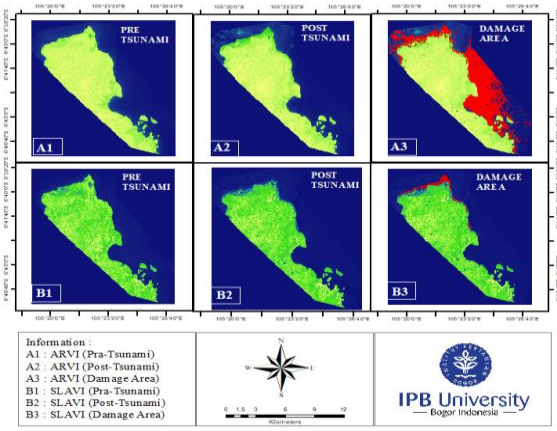

Figure 7. Index Assessment ARVI and SLAVI

ARVI index has a relatively high detection result (Figure 4). In this index, the larger affected area is distributed in the ocean area (Figure 7). The ARVI index is sensitive to atmospheric conditions, so it has a strong influence on this identification process (Kaufman and Tanre 1992). The SLAVI index was developed specifically to monitor vegetated objects with a level of leaf area sensitivity (Rahmawati *et al.* 2022). The SLAVI index spatially shows the affected area with a bluish color and has a blue color gradient that projects the severity of the tsunami-affected area. This is supported by the ability of the SLAVI index to be more sensitive to the leaf area (Lymburner *et al.* 2000), thus forming a color gradation in the detection results. The difference between ARVI and SLAVI indices can be used to map a type of land use that is reviewed from the wavelength of an object from various indices received by satellites.

Green Normalized Difference Vegetation Index (GNDVI) was developed to assess the variability of leaf chlorophyll when the leaf area index is high enough (Gitelson *et al.* 1996). GNDVI only produces an area of 254.69 ha or equivalent to 0.20% of the total area of UKNT conservation areas (Table 5). The GNDVI

index is associated with the chlorophyll content of the leaves so it is sensitive to the level of plant density around the affected area (Shanahan *et al.* 2001). Gianelle *et al.* (2009) assert that GNDVI is less affected by saturation. A number of optical satellite sensors acquire data at the spectral wavelengths needed to produce this vegetation index at the pixel level. The soil adjusted vegetation index (SAVI) shows that the distribution of damage due to the tsunami is 0.02% greater when compared to the GNDVI index, where the area of damage identified is 272.82 ha. SAVI is a vegetation index whose calculation is adjusted to open land cover to minimize the effects of poor vegetation cover (Jorge *et al.* 2019). Overall. although SAVI shows higher sensitivity, both indices can be used to assess the extent of damage to vegetation land caused by a disaster (Zhou *et al.* 2016).

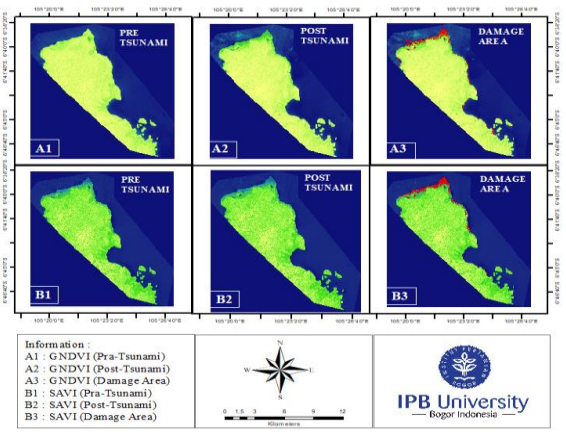

Figure 8. Index Assessment GNDVI and SAVI

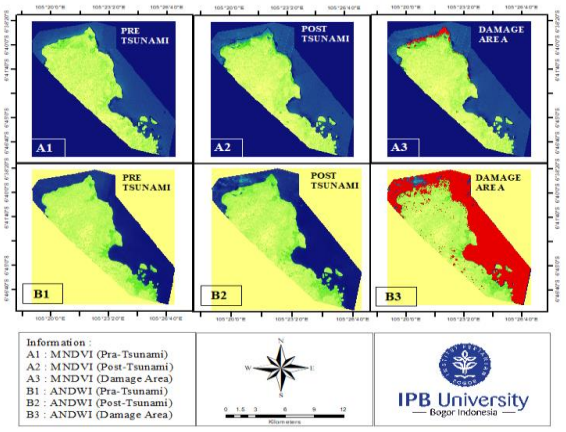

Figure 9. Index Assessment MNDVI and ANDWI

Index Assessment *maximum normalized difference vegetation index* (MNDVI) and *augmented normalized difference water index* (ANDWI) to the distribution of the extent of damage before, after, and the affected area (Figure 9). MNDVI demonstrated the maximum ability of vegetation to absorb photosynthetically active radiation (PAR) (Fu *et al.* 2013). The variation of MNDVI depends on the type of vegetation and climatic conditions in a region (Shen *et al.* 2014). The distribution of damage shown by MNDVI was 207.01 ha or about 0.16% of the overall study area marked in red in the northwest to the north of the study area. There was a significant difference in the affected area from the two indices above, where ANDWI showed a larger affected area of 5.09% of the study area or equivalent to 6269.35 ha spread from northwest to southeast in the water body of the study area. This is because ANDWI was developed based on comprehensive experiments on spectral characteristics to separate water bodies from other land covers, given that tsunami events will also cause damage to water bodies that have direct contact (Otsu 1979; Prost *et al.* 2008; Vos *et al.* 2019). ANDWI can correctly identify water bodies even if the imagery used is disturbed by clouds because it applies the principle of higher SWIR channel reflectance to true color (RGB) map conditions (Rad *et al.* 2021).

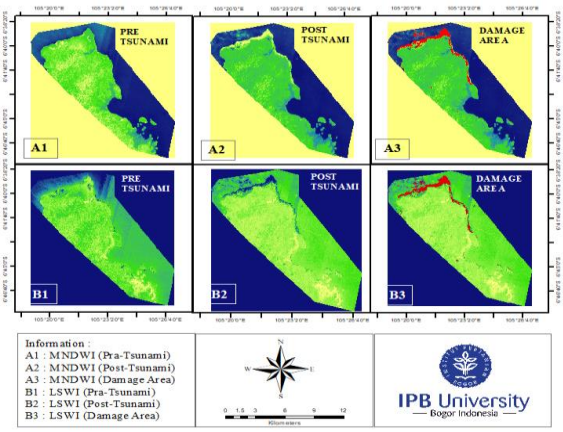

Figure 10. Index assessment MNDWI and LSWI

Modified normalized difference water index (MNDWI) dan *land surface water index* (LSWI) is an index used to describe the area of water bodies or land cover containing water. MNDWI has a high level of sensitivity in showing water content in built-up lands while LSWI is used to estimate ground-level water content (Xu 2006; Xiao *et al.* 2022). The visualization of the area of damage described by MNDWI and LSWI did not have a significant difference, where the damage depicted was 0.35% (435.88 ha) and 0.33% (415.61 ha) of the study area, respectively. The pattern of distribution of damage is the same, namely from the northwest to the southeast

of the study area. Jiang *et al.* (2022) stated that MNDWI can also show water information on various land cover including vegetation under different growing conditions using blue bands. The LSWI index can identify flooding by applying the relationship of land cover change described by NDVI and EVI, but cannot distinguish between water and vegetation so it is not recommended for vegetation classification (Giri *et al.* 2011; Dong *et al.* 2016). Overall, the two indices can separate water bodies in a small scope but there are drawbacks due to the excessive use of formula derivatives (Niu *et al.* 2022).

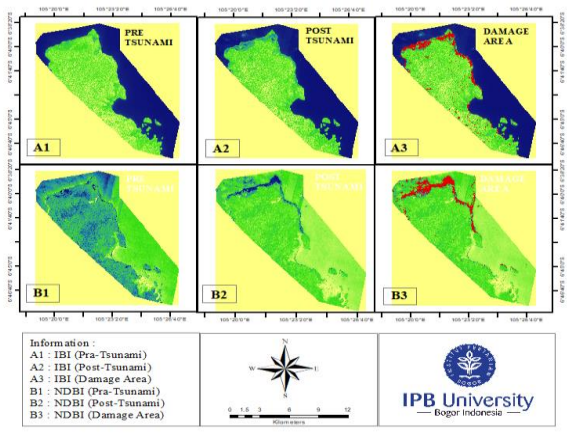

Figure 11. Index assessment IBI and NDBI

Normalized difference built-up index (NDBI) and *index-based built-up index* (IBI) is an index that is easy to use in describing the area of built-up land in an area. IBI is a derivative index of NDBI by combining SAVI and MNDWI as its calculation component (Li *et al.* 2017). Both NDBI and IBI can describe areas with impermeable surfaces without omitting information regarding water bodies (Chen *et al.* 2020). The distribution of the area of tsunami damage described by the NDBI was greater, namely 0.54% or 667.5 ha when compared to IBI with an area of about 0.49% or 606.65 ha from the overall study area. NDBI is used to describe built-up land (urban area) while IBI can represent three main components, namely built-up land, vegetation, and water in an area (Sekertekin *et al.* 2018). In urban landscapes, NDBI excels at representing variations in thermal acceptance and surface moisture (Essa *et al.* 2012; Wang *et al.* 2020).

Index Testing Accuracy

All indices have different characteristics so they are expected to provide recommendations for methods that can be trusted and shown with a degree of accuracy. The results of the analysis show that spatial information regarding the impact of the tsunami can be received with a fairly high level of accuracy. The assessment of accuracy results refers to the OA and KS values. Fitzgerald and Lees (1994) explain that the process of misclassification can be seen from the value of KS. This is shown by the highest OA and KS values in the MNDWI index, namely 98% and 0.96 (Table 6). In addition, there are other indices that have a fairly high level of accuracy and are smaller than the MNDWI index. The indices are SLAVI, SAVI, and NDVI indices which have OA and KS values of 94% and 0.89. According to Scepan (1999), an acceptable accuracy value is shown with an OA value that ranges above 85%. Therefore, of the 12 indices tested, only 7 indexes have an OA accuracy value above 85%. These indices include MNDWI, SLAVI, SAVI, NDVI, MNDVI, EVI, and LSWI. Meanwhile, other indices only have accuracy values below that threshold. The 85% figure in the assessment of accuracy results is a limiter for the feasibility of spatial information resulting from the classification process and is often used by several previous researchers/authors (Foody 2008).

The lowest accuracy value is owned by the building type index, namely IBI with an OA value of 44% and KS of 0.26. The low accuracy value produced is influenced by the ability of the index to identify the earth's surface. The IBI index is generally used in identifying built-up land, so it is not suitable to be applied in identifying tsunami impacts in forest areas. However, the other building index involved, namely the NDBI, has an accuracy value of 82% for OA and 0.68 for KS. The difference in the resulting accuracy values of these two indices is influenced by the involvement of bands in the index formula. Therefore, this index has the potential to identify the impact of tsunamis in residential areas.

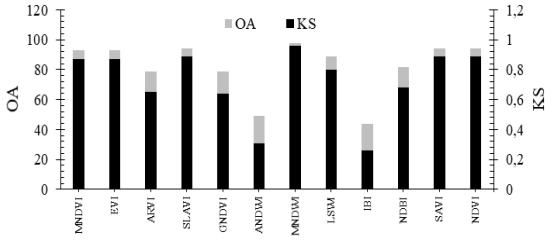

Figure 12. Accuracy assessment

CONCLUSIONS

Handeuleum Island is located on the Ujung Kulon Peninsula in the northern part of Banten, adjacent to the Krakatau Nature Reserve. The tsunami in 2018

caused damage to the peninsula of Ujung Kulon National Park. Geospatial technology in identifying the impact of disasters using Sentinel 2 type Multispectral Instrument (MSI) imagery. The area affected by the 2018 tsunami reached 1,268.53 ha. The MNDWI method has the highest accuracy rate, namely 98% (total accuracy) and 0.96 (kappa statistics) which are classified as precise and almost perfect. The analysis shows that the tsunami had a negative impact on coastal forest vegetation on the Ujung Kulon peninsula and surrounding settlements. Therefore, these problems need special attention, especially in the UKNP ecosystem. This study is expected to be a consideration for the management of the UKNP area within the framework of the existing ecosystem to protect the endangered Javan Rhino.

ACKNOWLEDGEMENTS

The authors thank the IPB SSRS Association which has facilitated the preparation of this scientific article. And thanks to The Osaka Gas Foundation for funding this research through The Osaka Gas Foundation of International Cultural Exchange (OGFICE) funding scheme, funding year 2021-2022.

REFERENCES

Adni SF, Asy'Ari R, Raihan F, Putra EI. 2024. Carbon stock estimation based on remote sensing in the northern coast of Java. *IOP Conference Series: Earth and Environmental Science*. 1315(1): 012042. https://doi.org/10.1088/1755-1315/1315/1/012042

Alwysihah H, Adni SF, Asy'Ari R. 2023. Mapping of Land Use in Cijengkol Village, Subang Regency Using Sentinel-2 MSI (MultiSpectral Instrument). *Jurnal Lahan Suboptimal: Journal of Suboptimal Lands*. 12(1):1-0. https://doi.org/10.36706/jlso.12.1.2023.627

Alongi DM. 2008. Mangrove forests: resilience, protection from tsunamis, and responses to global climate change. Estuarine, coastal and shelf science. 76(1):1-3. https://doi.org/10.1016/j.ecss.2007.08.024

Asy'Ari R, Alamako WB, Aslam MF, Nurhawaillah LE, Rivai FA, Pramulya R, Zamani NP, Setiawan Y. 2023A. Spatiotemporal for Sea Reclamation in Makassar City Coastline, South Sulawesi: Best Solution or Environmental Impact?. *DataBrief*. 1:1-4

Asy'Ari R, Ranti A, Rahmawati AD, Zulfajrin M, Nurazizah LL, Putra MC, Khairunnisa ZN, Prameswari FA, Pramulya R, Zamani NP, Setiawan Y. 2023B. High heterogeneity LULC classification in Ujung Kulon National Park, Indonesia: A study testing 11 indices, Random Forest, sentinel-2 MSI, and GEE-based cloud computing. *Celebes Agricultural*. 3(2):82-99. https://doi.org/10.52045/jca.v3i2.381

Chen J, Chen S, Yang C, He L, Hou M, Shi T. 2020. A comparative study of impervious surface extraction using Sentinel-2 imagery. *European Journal of Remote Sensing*. 53(1): 274-292. https://doi.org/10.1080/22797254.2020.1820383

Congalton R & Green K. 2019. *Assessing the Accuracy of Remotely Sensed Data Principles and Practices*, Third Edition. United States: CRC Press https://doi.org/10.1201/9781420055139

Drusch M, Del Bello U, Carlier S, Colin O, Fernandez V, Gascon F, Hoersch B, Isola C, Laberinti P, Martimort P, Meygret A. 2012. Sentinel-2: ESA's optical high-resolution mission for GMES operational services. *Remote sensing of Environment*. 120:25-36. https://doi.org/10.1016/j.rse.2011.11.026

Dong J, Xiao X, Menarguez MA, Zhang G, Qin Y, Thau D, Biradar C, Moore B. 2016. Mapping paddy rice planting area in Northeastern Asia with Landsat 8 images, phenology-based algorithm and Google Earth Engine. *Remote Sensing of Environment*. 185: 42–154. https://doi.org/10.1016/j.rse.2016.02.016

Essa WB, Verbeiren, J. van der Kwast T. Van de Voorde O. Batelaan. 2012. Evaluation of the DisTrad Thermal Sharpening Methodology for Urban Areas. International *Journal of Applied Earth Observation and Geoinformation,* 19: 163–172. https://doi.org/10.1016/j.jag.2012.05.010

Fitzgerald RW, Lees BG. 1994. Assessing the classification accuracy of multisource remote sensing data. *Remote sensing of Environment*. 47(3):362-8. https://doi.org/10.1016/0034-4257(94)90103-1

Fu G, Shen ZX, Sun W, Zhong ZM, Zhang XZ, Zhou YT. 2015. A meta-analysis of the effects of experimental warming on plan physiology and growth on the Tibetan Plateau. Journal of Plant Growth Regulation. 34: 57–65. https://doi.org/10.1007/s00344-014-9442-0

Foody GM. 2004. Thematic map comparison: evaluating the statistical significance of differences in classification accuracy. *Photogrammetric Engineering & Remote Sensing*. 70(5): 627–633.

Foody GM. 2008. Harshness in image classification accuracy assessment. *International Journal of Remote Sensing*. 29(11): 3137-3158. http://dx.doi.org/10.1080/01431160701442120

Gitelson AA., Kaufman YJ, Merzlyak MN. 1996. Use of a green channel in remote sensing of global vegetation from EOS-MODIS. *Remote Sensing of Environment*. 58: 289–298. https://doi.org/10.1016/S0034-4257(96)00072-7

Gianelle D, Vescovo L, Marcolla B, Manca G, Cescatti A. 2009. Ecosystem carbon fluxes and canopy spectral reflectance of a mountain meadow. *International Journal of Remote Sensing*. 30:435–449. https://doi.org/10.1080/01431160802314855

Giri C, Ochieng E, Tieszen LL, Zhu Z, Singh A, Loveland T, Masek J, Duke N. 2011. Status and distribution of mangrove forests of the world using earth observation satellite data. *Global Ecology and Biogeography*. 20(1): 154-159. https://doi.org/10.1111/j.1466-8238.2010.00584.x

Gorelick N, Hancher M, Dixon M, Ilyushchenko S, Thau D, Moore R. 2017. Google Earth Engine: Planetary-scale geospatial analysis for everyone. *Remote sensing of Environment*. 202:18-27. https://doi.org/10.1016/j.rse.2017.06.031

Hommel PW. 1987. *Landscape-ecology of Ujung Kulon* (*West Java, Indonesia*). Wageningen University and Research.

Huete, A.R., 1988. A soil-adjusted vegetation index (SAVI). *Remote Sensing of Environment*. 25 (3): 295–309. https://doi.org/10.1016/0034-4257(88)90106-X

Jiang Z, Wen Y, Zhang G, Wu X. 2022. Water Information Extraction Based on Multi-Model RF Algorithm and Sentinel-2 Image Data. *Sustainability* 2022, 14: 3797. https://doi.org/10.3390/su14073797

Jorge J, Vallbé M, Soler JA. 2019. Detection of irrigation inhomogeneities in an olive grove using the NDRE vegetation index obtained from UAV images. *European Journal of Remote*

Sensing, 52(1): 169-177. https://doi.org/10.1080/22797254.2019.1572459

Kaufman YJ, Tanre D. 1992. Atmospherical resistant vegetation index (ARVI) for EOSMODIS. IEEE Transactions on Geoscience and Remote Sensing. 30:261-270. https://doi.org/10.1109/36.134076

Kumar L, Mutanga O. 2018. Google Earth Engine applications since inception: Usage, trends, and potential. Remote sensing. 10(10):1509. https://doi.org/10.3390/rs10101509

Koshimura S, Moya L, Mas E, Bai Y. 2020. Tsunami damage detection with remote sensing: A review. *Geosciences*. 10(5):177. https://doi.org/10.3390/geosciences10050177

Lymburner L, Beggs PJ, Jacobson CR. 2000. Estimation of canopy-average surface-specific leaf area using Landsat TM data. *Photogrammetric Engineering and Remote Sensing* 66, 183–191.

Abd Malik AM, Jouhary NA, Ulfa A, Rahmadhanti IN, Pudjawati NH, Asy'Ari R, Zamani NP, Pramulya R, Setiawan Y. 2024. Monitoring of coastal dynamics at Subang Regency using Landsat Collection Data and Cloud Computing Based. *BIO Web of Conferences*. 106: 04005. https://doi.org/10.1051/bioconf/202410604005

Marlier ME, Resetar SA, Lachman BE, Anania K, Adams K. 2022. Remote sensing for natural disaster recovery: Lessons learned from Hurricanes Irma and Maria in Puerto Rico. *Environmental Science & Policy*. 132:153-9. https://doi.org/10.1016/j.envsci.2022.02.023

Marine Protected Areas in South East Asia. 2005. Available online at: http://www.arcbc.org.ph/BISS/MarinePA/idn.htm.

Muhari A, Heidarzadeh M, Susmoro H, Nugroho HD, Kriswati E, Supartoyo, Wijanarto AB, Imamura F, Arikawa T. 2019. The December 2018 Anak Krakatau volcano tsunami as inferred from post-tsunami field surveys and spectral analysis. *Pure and Applied Geophysics*. 176:5219-33. https://doi.org/10.1007/s00024-019-02358-2

Mutanga O, Kumar L. 2019. Google earth engine applications. *Remote sensing*. 11(5):591. https://doi.org/10.3390/rs11050591

Navarro G, Caballero I, Silva G, Parra PC, Vázquez Á, Caldeira R. 2017. Evaluation of forest fire on Madeira Island using Sentinel-2A MSI imagery. *International Journal of Applied Earth Observation and Geoinformation*. 58:97-106. https://doi.org/10.1016/j.jag.2017.02.003

Niu L, Kaufmann H, Xu G, Zhang G, Ji C, He Y, Sun M. 2022. Triangle Water Index (TWI): An Advanced Approach for More Accurate Detection and Delineation of Water Surfaces in Sentinel-2 Data. *Remote Sensing*. 14: 5289. https://doi.org/10.3390/rs14215289

Otsu N. 1979. A threshold selection method from gray-level histograms. IEEE Trans.Syst., Man, Cybernet, 9 (1): 62–66.

Prost CJ, Dare PM, Zerger AZ. 2008. Discrimination of Eucalyptus canopy from airborne linescanner imagery using Markov random field modelling. Environmental Modelling & Software. 23 (1): 56–71. https://doi.org/10.1016/j.envsoft.2007.05.001

Pettorelli N, Vik JO, Mysterud A, Gaillard JM, Tucker CJ, Stenseth, NC. 2005. Using the satellite-derived NDVI to assess ecological responses to environmental change. *Trends in ecology & evolution*. 20(9): 503-510. https://doi.org/10.1016/j.tree.2005.05.011

Rad AM, Kreitler J, Sadegh M. 2021. Augmented normalized difference water index for improved surface water monitoring. *Environmental Modelling & Software*. 140:1-15. https://doi.org/10.1016/j.envsoft.2021.105030

Rafliana I, Jalayer F, Cerase A, Cugliari L, Baiguera M, Salmanidou D, Necmioğlu Ö, Ayerbe IA, Lorito S, Fraser S, Løvholt F. Tsunami risk communication and management: Contemporary gaps and challenges. *International Journal of Disaster Risk Reduction*. 70:102771. https://doi.org/10.1016/j.ijdrr.2021.102771

Rahmawati, Azelia Dwi, Rahmat Asy'Ari, Muhammad Aqbal Fathonah, Neviaty Putri Zamani, Rahmat Pramulya, and Yudi Setiawan. 2022. Vegetation-Water-Built Up Index Combined: Algorithm Indices Combination for Characterization and distribution of Mangrove Forest through Google Earth Engine: *CELEBES Agricultural*. 3(1): 20-42. https://doi.org/10.52045/jca.v3i1.298

Rajan SC, Dominic L, Vishnu M, Athira K, Sooraj NP, Jaishanker R. 2022. Surrogacy of post natural disaster acoustic indices for biodiversity assessment. *Environmental Challenges*. 6:100420. https://doi.org/10.1016/j.envc.2021.100420

Rees G. 1999. *The Remote sensing Data Book*. England: Cambridge University Press.

Rivai FA, Asy'Ari R, Fadhil MH, Jouhary NA, Saenal N, Ardan F, Pohan A, Pramulya R, Setiawan Y. 2023. Analysis of Land Use Land Cover Changes using Random Forest through Google Earth Engine in Depok City, Indonesia. *SSRS Journal B: Spatial Research*. 1: 01-12 https://publishing.ssrs.or.id/ojs/index.php/ssrs-b/article/view/7

Rouse jr JW, Haas RH, Schell JA & Deering DW. 1974. Monitoring vegetation systems in the Great Plains with ERTS. *NASA special publication*. 351(1974): 309

Rwanga SS, Ndambuki JM. 2017. Accuracy assessment of land use/land cover classification using remote sensing and GIS. *International Journal of Geosciences*. 8(04):611. https://doi.org/10.4236/ijg.2017.84033

Sambah AB, Miura F. 2016. Spatial data analysis and remote sensing for observing tsunami-inundated areas. International Journal of Remote Sensing. 37(9):2047-65. http://dx.doi.org/10.1080/01431161.2015.1136450

Santiapillai C, Suprahman H . 1986. The proposed translocation of the Javan rhinoceros Rhinoceros sondaicus. Biological Conservation. 38: 11–19. https://doi.org/10.1016/0006-3207(86)90016-9

Scepan J. 1999. Thematic validation of high-resolution global land-gover data sets. *Photogrammetric Engineering & Remote Sensing*. 65(9): 1051-1060.

Sekertekin A, Abdikan S, Marangoz AM. 2018. The acquisition of impervious surface area from LANDSAT 8 satellite sensor data using urban indices: a comparative analysis. *Environmental monitoring and assessment*. 190(7): 1-13. https://doi.org/10.1007/s10661-018-6767-3

Seydi ST, Akhoondzadeh M, Amani M, Mahdavi S. 2021. Wildfire damage assessment over Australia using sentinel-2 imagery and MODIS land cover product within the google earth engine cloud platform. *Remote Sensing*. 13(2):220. https://doi.org/10.3390/rs13020220

Shanahan JF, Schepers JS, Francis DD, Varvel GE, Wilhelm W. 2001. Use of remote-sensing imagery to estimate corn grain yield. *Agronomy Journal*. 93(3):583–589. https://doi.org/10.2134/agronj2001.933583x

Shen Z, Fu G, Yu C, Sun W, Zhang X. 2014. Relationship between the growing season maximum enhanced vegetation index and climatic factors on the Tibetan Plateau. *Remote Sensing*. 6: 6765–6789. https://doi.org/10.3390/rs6086765

Singh KK, Nigam MJ, Pal K. 2014. Detection of 2011 Tohoku tsunami inundated areas in Ishinomaki City using generalized improved fuzzy Kohonen clustering network. European Journal of Remote Sensing. 47(1):461-75. https://doi.org/10.5721/EuJRS20144726

Somvanshi SS, Kumari M. 2020. Comparative analysis of different vegetation indices with respect to atmospheric particulate pollution using sentinel data. *Applied Computing and Geosciences*. 7: 100032. https://doi.org/10.1016/j.acags.2020.100032

The Indonesian Nature Conservation Database. Available online at: http://users.bart.nl/~edcolijn/kulon.html.

UNESCO-WHC (World Heritage Centre). Case study 6. Ujung Kulon National Park – Indonesia. Available online at: http://whc.unesco.org/pg.cfm?cid=286.

Vos K, Splinter KD, Harley MD, Simmons JA, Turner IL. 2019. CoastSat: a Google Earth Engine-enabled Python toolkit to extract shorelines from publicly available satellite imagery. *Environmental Modelling & Software*. 122: 104528. https://doi.org/10.1016/j.envsoft.2019.104528

Xiao X, Boles S, Frolking S, Salas W, Moore B, Li C, He L, Zhao R. 2002. Observation of flooding and rice transplanting of paddy rice fields at the site to landscape scales in China using vegetation sensor data. *International Journal of Remote Sensing*. 23: 3009–3022. https://doi.org/10.1080/01431160110107734

Xu H. 2006. Modification of normalised difference water index (NDWI) to enhance open water features in remotely sensed imagery. *International Journal of Remote Sensing*. 27 (14): 3025–3033. https://doi.org/10.1080/01431160600589179

Xu H. 2008. A new index for delineating built-up land features in satellite imagery. *International Journal of Remote Sensing*. 29(14): 4269–4276. https://doi.org/10.1080/01431160802039957

Wandani RA, Asy'Ari R, Setiawan Y, Anggodo A. Deteksi ekspansi padi pada lanskap hutan di Taman Nasional Ujung Kulon, Indonesia menggunakan algoritma RF dan Sentinel-2 multispectral instrumen. *National Multidisciplinary Sciences*. 1(2):235-45. https://doi.org/10.32528/nms.v1i2.64

Wang JW, Chow WT, Wang YC. 2020. A global regression method for thermal sharpening of urban land surface temperatures from MODIS and Landsat. *International journal of remote sensing*. 41(8): 2986-3009. https://doi.org/10.1080/01431161.2019.1697009

Wardlow BD, Anderson MC, Sheffield J, Doorn BD, Verdin JP, Zhan X, Rodell M. 2012. Future Opportunities and Challenges in Remote Sensing of Drought. *Remote Sensing of Drought: Innovative Monitoring Approaches*. CRC Press. 389. https://doi.org/10.1201/b11863

Wells, Michael & Guggenheim, Scott & Khan, Asmeen & Wardduo, Wahjude & Jepson, Paul. 1999. Investing in biodiversity. A Review of Indonesia's Integrated Conservation and Development Projects.

Zha Y, Gao J, Ni S. 2003. Use of normalized difference built-up index in automatically mapping urban areas from TM imagery. *International Journal of Remote Sensing*. 24(3): 583-594. https://doi.org/10.1080/01431160304987

Zhou J, Mark J. Pavek, Seth C. Shelton, Zachary J. Holden, Sindhuja Sankaran. 2016. Aerial multispectral imaging for crop hail damage assessment in potato. *Computers and Electronics in Agriculture*. 127: 406-412. https://doi.org/10.1016/j.compag.2016.06.019

Zia U, Riaz MM, Ghafoor A. 2022. Transforming remote sensing images to textual descriptions. *International Journal of Applied Earth Observation and Geoinformation*. 108:102741. https://doi.org/10.1016/j.jag.2022.102741

Zeng Y, Hao D, Huete A, Dechant B, Berry J, Chen JM, Joiner J, Frankenberg C, Bond-Lamberty B, Ryu Y, Xiao J. 2022. Optical vegetation indices for monitoring terrestrial ecosystems globally. *Nature Reviews Earth & Environment*. 3(7):477-93. https://doi.org/10.1038/s43017-022-00298-5